Ninth International Conference on Computational Fluid Dynamics (ICCFD9), Istanbul, Turkey, July 11-15, 2016

ICCFD9-xxxx

A Two-Dimensional Spectral Model of Blood Plasma Flow with Oxygen Transport and Blood Cell Membrane Deformation

G. Bueno[1], W. Harris[2]

[1]2015 Summer Research Assistant - Department of Aeronautics and Astronautics, Massachusetts Institute of Technology, Cambridge, MA, US
[2] Professor of Aeronautics and Astronautics, Massachusetts Institute of Technology, Cambridge, MA, USA

Corresponding author: gbuenolu@mit.edu

Abstract: Sickle cell disease (SCD) is a hereditary blood disorder in which the red blood cells (RBC) have abnormal cell structure and function. These abnormal RBC cannot efficiently transport and release oxygen as in a normal cell. In this investigation spectral methods in a 2-D computational model of flow dynamics are implemented in order to simulate plasma velocities, oxygen diffusion, and RBC deformation in the microcirculation. A mixed Chebyshev and Fourier spectral scheme with finite difference scheme is used to compute the flow field, oxygen diffusion, and RBC deformation. A level set computational method is used to advect the RBC membrane on a staggered grid. Simulations are made to compare the computed profiles with the results obtained by Tekleab and Harris [1]. Differences in profiles are discussed and both sets of profiles are compared with the three-dimensional model of Le Floch-Yin [2].

Keywords: Microcirculation, Sickle Cell, Red Blood Cell, Spectral Methods, Pseudospectral Methods, Finite Difference, Level Set, Chebyshev Polynomials, Blood Plasma Flow, Oxygen Diffusion.

1 Introduction

In order to increase the knowledge of human blood flow in the capillaries, mathematical models may be useful. In the case of diseases such as Leukemia, malaria and sickle cell anemia models that capture the affect of physiological parameters are novel. Sickle cell disease [SCD] is a genetic disorder that is caused by sickle-shaped red blood cells [RBC] that clog capillaries in humans. It is characterized by a state of anemia, or a deficiency of hemoglobin, which alters the structure of the RBC or erythrocytes. Consequently, the blood plasma dynamics, blood cell deformation and convection, oxygen diffusion across the membrane of RBC and the transport of oxygen into the blood plasma and the surrounding tissue is compromised. Le Floch-Yin [2] has developed an unsteady three-dimensional systemic macroscopic model of human blood flow with a sickle and normal cell deformation and oxygen deformation in the capillaries. Tekleab [3] has also developed a two-dimensional, three-layers of the same problem with great results when compared to Le Floch-Yin results. In both cases finite differences schemes were used for implementing the model. In this report we detail the development and implementation of a mixed spectral-finite differences scheme to mathematically model the unsteady two-dimensional human blood plasma flow with oxygen transport and blood cell membrane deformation. Computed profiles are compared with other published data.

2 Problem Statement

With the same ambition of simplicity in a systemic macroscopic two-dimensional model, the 3-layer model of the physical system [3] is used instead of 5-layers model as Le Floch-Yin [2], that results in a higher computational costs. The 5-layers model of LeFloch-Yin [2] was neglected due to the large amount of RBCs and plasma in the 5-layers model and the requirement for consistence when the analyzing the smallest blood vessels or capillaries with one cell thickness.

Therefore, for our computational domain is considered the RBC membrane, blood plasma and surrounding tissue (3-layer model), which is depicts in Figure 1.

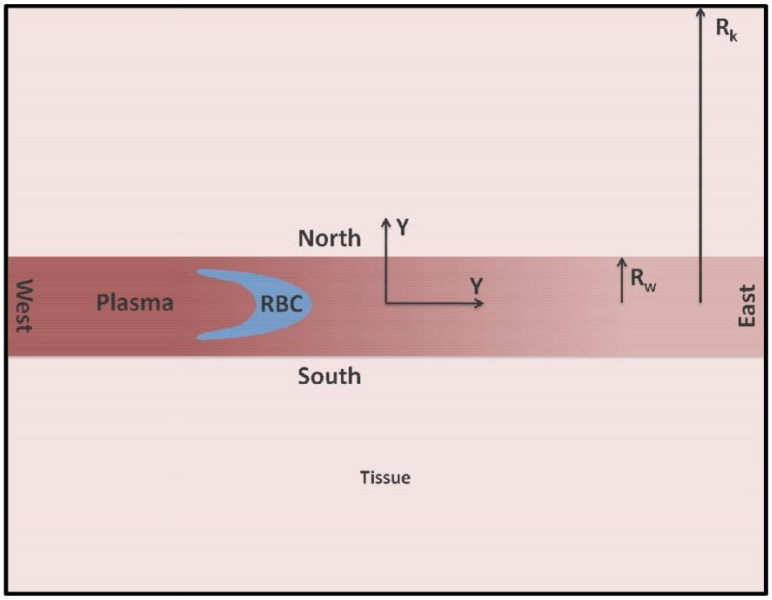

Figure 1: 3-Layer Capillary Model[1]

In this model the microcirculation system is considered an isothermal and incompressible blood plasma flow, with Navier-Stokes as a governing equation accounting for the conservation of mass. To begin the mathematical model, we will use the following set of governing fluid dynamics equations: (1) Continuity equation, (2) Navier-Stokes equation and (3) Frick's Law of mass diffusion to deal with the diffusion and transport of oxygen.

$$\nabla \cdot \underline{v} = 0 \quad (1)$$

$$\rho\left(\frac{\partial \underline{v}}{\partial t} + \underline{v} \cdot \nabla \underline{v}\right) = -\nabla p + \mu \nabla^2 \underline{v} \quad (2)$$

$$\frac{\partial c}{\partial t} + \nabla \cdot \left(c\underline{v} - D_{ox}\nabla c\right) = R(c) \quad (3)$$

3 Computational Model

The blood plasma flow conditions is based on a two dimensional Navier-Stokes equations, which have been reduced to vorticity-stream function form. For the implementation, Chebyshev polynomials are used in inhomogenous and Fourier spectral scheme in homogeneous direction [4]. Initially with non-slip boundary condition, differentiation matrices solve the system of equations. In order to handle the physical geometry of the problem, a pseudospectral "staggered" grid is used. The oxygen concentration calculations are based in a finite differences scheme developed by Tekleab [3].

3.1 Blood Plasma Flow

The blood plasma flow is mathematically represented by the two-dimensional incompressible form of Navier-Stokes equation (2) and (3). The dimensionless form of these equations is given by:

$$\frac{\partial u}{\partial t} + u\frac{\partial u}{\partial x} + v\frac{\partial u}{\partial y} - \frac{1}{Re}\Delta u = -\frac{\partial p}{\partial x} \quad (4)$$

$$\frac{\partial v}{\partial t} + u\frac{\partial v}{\partial x} + v\frac{\partial v}{\partial y} - \frac{1}{Re}\Delta v = -\frac{\partial p}{\partial y} \quad (5)$$

Differentiating eq. (4) with respect to y and eq. (5) with respect to x and adding them, we obtain the vorticity-streamfunction formulation. Keeping in mind that the streamfunction ψ and vorticity ω are defined by:

$$\mathrm{u} = \frac{\partial \psi}{\partial \mathrm{y}}, \mathrm{v} = -\frac{\partial \psi}{\partial \mathrm{x}}, \omega = \frac{\partial \mathrm{u}}{\partial \mathrm{x}} - \frac{\partial \mathrm{u}}{\partial \mathrm{y}} \quad (6)$$

Therefore, the system of equation in the vorticity form with Poisson equation is shown bellow:

$$\frac{\partial \omega}{\partial t} = \frac{\partial \psi}{\partial x}\frac{\partial \omega}{\partial y} - \frac{\partial \psi}{\partial y}\frac{\partial \omega}{\partial x} + \nu\left(\frac{\partial^2 \omega}{\partial x^2} + \frac{\partial^2 \omega}{\partial y^2}\right) \quad (7)$$

$$\omega = -\left(\frac{\partial^2 \psi}{\partial x^2} + \frac{\partial^2 \psi}{\partial y^2}\right) \quad (8)$$

3.2 Spatial and Time Discretization

Pseudospectral methods are the most flexible and easiest among all spectral methods for implementation and afford spectral convergence for smooth solutions [5]. The main idea is to choose a set of collocation points for a given grid, making the residual function to be zero at this new points. Moreover an interpolate polynomial must be chosen to fit those values. The selection of it is based on the *sampling theorem* which says that there are infinite possible interpolate for any grid, but there is only one band-limited interpolant defined in a specific case [6].

In order to create the differentiation matrices, the unknown function $u(x)$ with $n+1$. Collocation points $\{x_j\}_{j=0}^{n}$ has the interpolating polynomial

$$P_n u(x) = \sum_j^{n-1} u(x_j)\, q_j(x) \quad (9)$$

Where $q_j(x)$ are the polynomials, which satisfy the *Kronecker delta function*. To obtain an approximation of s-order derivation for the function $u(x)$, we must derive s times at the collocation points. The pseudospectral approximation is shown bellow:

$$\frac{d^s P_n u(x_k)}{dx^s} = \sum_j^{n-1} u(x_j) \left[\frac{d^s}{dx^s} q_j(x)\right]_{xk} = \sum_j^{n-1} u(x_j)\, D_{kj}^{(s)} \quad (10)$$

where $D_{kj}^{(s)}$ are the entries of the s-order differentiating matrix $D^{(s)}$.

In our case, for the homogeneous direction is Fourier collocation method is used. After domain corrections and known that this domain is a subset of the interval $[0,2\pi]$, we have:

$$P(x) = \frac{h}{2\pi} \sum_{k=-N/2}^{N/2} e^{ikx} = \frac{h}{2\pi} \cos(x/2) \frac{\sin(Nx/2)}{\sin(x/2)} \quad (11)$$

The number of collocation points is given by odd number N, in this way, the spacing of the grid points is $h = 2\pi/N$ and consequently we can write $P(x)$ dependent of a periodic *sinc function*

$$S_N(x) = \frac{\sin(\pi x/h)}{(2\pi/h)\tan(x/2)} \quad (12)$$

which gives us the entries of the 1^{st}order differentiation matrix D_N:

$$S'_N(x_j) = \begin{cases} 0 & j \equiv 0 \ (mod\ N) \\ \frac{1}{2}(-1)^j \cot(jh/2) & j \not\equiv 0 \ (mod\ N) \end{cases}$$

Analogous, it is possible to write the 2^{nd}order differentiation matrix $Df_N^{(2)}$ entries

$$S''_N(x_j) = \begin{cases} -\frac{\pi^2}{3h^2} - \frac{1}{6} & j \equiv 0 \ (mod\ N) \\ -\frac{(-1)^j}{2\sin^2(jh/2)} & j \not\equiv 0 \ (mod\ N) \end{cases}$$

As those are *Toeplitz* matrices, having constant entries along diagonals, their construction and implementation is easier.
In spectral methods when working with algebraic polynomials, an irregular grid with asymptotic spacing must be used; otherwise, the catastrophic *Runge Phenomenon* appears. In this phenomenon, the discretization not only fails to converge as $N \to \infty$, but also, get worse at a rate 2^N [6].

For those reasons, in the homogeneous direction, the so-called Chebyshev Gauss-Lobatto collocation points [7], defined on the entire interval $[-1, 1]$ is used. In addition, the interpolate polynomial $P(X)$ is initially written in the Lagrange form in order to satisfy the initial and final points in the interval, $x_0 = -1$ and $x_1 = 1$ respectively. Interpolating through data v_0 and v_1 as an example with $N = 1$:

$$P(x) = \frac{1}{2}(1+x)v_0 + \frac{1}{2}(1-x)v_1 \Longrightarrow P'(x) = \frac{1}{2}v_0 - \frac{1}{2}v_1$$

where $P'(x)$ is the derivate of the interpolating polynomial. Therefore, the 1^{st}order differentiation matrix can be written as:

$$Dc_1 = \begin{pmatrix} \frac{1}{2} & -\frac{1}{2} \\ \frac{1}{2} & -\frac{1}{2} \end{pmatrix} \quad (13)$$

Expanding for a N^{th} order differentiation matrix, it is possible to obtain the following entries for this matrix:

$$(Dc_N)_{kj} = \begin{cases} \frac{(-1)^{k+j}}{x_k - x_j}\frac{a_k}{a_j}, & k \neq j \\ \frac{-x_k}{2(1-x_k^2)}, & 1 \leqq k = j \leqq N-1 \\ \frac{2N^2+6}{6}, & k = j = 0 \\ -\frac{2N^2+6}{6}, & k = j = N` \end{cases},$$

$$where: \quad a_j = \begin{cases} 2, & j = 0, N \\ 1, & 1 \leqq j < N \end{cases} \quad and \quad a_j = \cos(j\pi/N)$$

The 2^{nd} order Chebyshev differentiation matrix can be obtained by simple matrix operation

$$Dc_N^{(2)} = \left(Dc_N^{(1)}\right)^2$$

It is important to mention that this integer N has not the same restriction as it has in interpolation Fourier, it can be even or odd. The matrix Dc_N of order N has a size $(N+1)$ x $(N-1)$.

In this report both Df and Dc are linear operators, they are used in the discretization of eq (7) and (8) as follows:

$$\frac{\partial \omega}{\partial t} = Df_N^{(1)}(\psi_i)Dc_N^{(1)}(\omega_i) - Dc_N^{(1)}(\psi_i)Df_N^{(1)}(\omega_i) + vL_N(\omega_i) \quad (14)$$

$$\omega_{i+1} = -L_N(\psi_i) \quad (15)$$

Where L_N is the Laplacian operator. As mentioned before, those differentiation matrices are linear operators and in order to convert those to become a bilinear operators, which is the case of the Laplacian operator, the *tensor product* is requested setting a grid base on Chebyshev and Fourier points independently in each direction. However, this can be a wasteful process and among the various technics to reduce the waste, the tensor product in linear algebra, known as *Kronecker product* is used.

To explain the main idea of the technic, lets consider matrices A and B with dimensions $m \times n$ and $p \times q$ respectively, the *Kronecker product* of those two matrices is represented by $A \otimes B$ this new matrix of dimensions $mp \times nq$ with $m \times n$ block form. Now, with tensor product spectral grid, it is possible to discretize the Laplacian operator L_N as:

$$L_N = I \otimes Dc_N^{(2)} + Df_N^{(2)} \otimes I \quad (16)$$

Where I is the identity matrix, used reorder the terms.

The L_N is not a sparse matrix, as the ones usually obtained in finite differences or finite elements. Even with a computational cost, the high accuracy of spectral methods make worth using this technic to construct our operator.

For stability and convergence of the solution, it is requested to handle with the CFL condition for the concentration of oxygen calculation in finite differences form, the unequal spacing grid in both x and y direction and the method of lines conditions for solving the time stepping. The basic idea of method of lines is solving coupled systems of ODEs in a finite differences form, with the *rule of thumb* as a criterion for stability.

Initially it was used an Euler discretization in time, but the computational time was decreasing the efficiency of the spectral method. We decided to work with the largest time step as possible without compromising the stability and convergence of the solution. Therefore, the *Adams-Bashforth* discretization is chosen for time stepping due to its large area of convergence and make possible to find an intersection point between all the requirements.

3.3 Flow Boundaries

As sketched in Figure 1, inflow boundary conditions were used on the west side and Neumann boundary condition on east side. For both north and south boundaries Dirichlet boundary conditions were used with the appropriate formulation for vorticity streamfunction formulation. In each time

step, the boundary conditions are calculated and updated in the Laplacian operator. As the Fourier-Chebyshev spectral grid is limited from $[-1,1]$ in y and periodic in x, boundaries were imposed in the correspondent index of the vorticiy ω. The staggered grid works with boundary conditions in a manner that some values are computed inside the cell. Therefore, similarly to Finite Volumes the boundary conditions are imposed with a help of the same concept of "*Ghost Cell "*.

3.4 RBC Membrane and Oxygen Diffusion

The level set method as developed by Tekleab [3] is used to model the RBC deformation, with a slight modification due to the Fourier-Chebyshev pseudospectral staggered scheme with different grid space in both directions and with cluster points in the north and south capillary walls. The major modification was in the jump matrix that corrects the velocity and pressure after the influence of the RBC membrane on the blood plasma flow.

Based on [7] the stiffness index (j) for sickle cell used is in the range $0 \leq j \leq 2$. Now, the relation between the RBC membrane deformation and the concentration of oxygen has a range of values for analysis based on the proposed Berger and King relation [7] between those:

$$\frac{k_{RBC}}{(k_{RBC})_0} = \left(\frac{c}{c_0}\right)^{-j} = \left(\frac{p_{o_2}}{(p_{o_2})_0}\right)^{-j}$$

Where $(k_{RBC})_0$ represents the stiffness of a normal cell; c_0 and $(p_{o_2})_0$ are the oxygen

concentration and oxygen partial pressure for a fully oxygenated cell at the arterial end of the capillary.

The Frick's Law of mass diffusion represented by eq (3) can be written in the computational domain as the following:

$$\frac{C^{n+1}-C^N}{\Delta t} + U^n C_x^n + V^n C_x^n - D_{ox}\left(C_{xx}^n + C_{yy}^n\right) = R(C^n)$$

Where R is the rate of hemoglobin O_2 production and myoglobin O_2 absorption and the relation between the myoglobin (S_{Mb}) and hemoglobin (S_{Hb}) saturation is computationally discretized as following:

$$R^n = k_{-1}^{Hb}[Hb]\left(S^{Hb^n} - \left(1 - S^{Hb^n}\right)\left(\frac{C^n}{C_{50\%}^{Hb}}\right)^n\right) + k_{-1}^{Mb}[Mb]\left(S^{Mb^n} - \left(1 - S^{Mb^n}\right)\left(\frac{C^n}{C_{50\%}^{Mb}}\right)^n\right) + M$$

Where M is the tissue O_2 consumption rate.

4 Results and Comparison

Our pseudospectral microcirculation numerical code was implemented to compare two basic cases with the already existed results for normal and sickle microcirculation. For distinguish one for the other, physiological parameters such as Hill coefficient, oxygen partial pressure at 50% hemoglobin saturation, arterial oxygen partial pressure and stiffness index are listed in the table bellow:

Table 1 – Microcirculation Cases Parameters

Parameters	**Normal Microcirculation**	**Sickle Microcirculation**
Hill coefficient (n)	2.7	3.0
p_{O_2} At 50% Hb saturation $\left(p_{O_{2,50\%}}^{Hb}\right)$	$3.33 \times 10^3 Pa$ $(25\ mmHg)$	$5.33 \times 10^3 Pa$ $(40\ mmHg)$
p_{O_2} In arteries $\left(p_{O_{2,50\%}}^{arterial}\right)$	$1.27 \times 10^3 Pa$ $(95\ mmHg)$	$1.07 \times 10^3 Pa$ $(80\ mmHg)$
Stiffness index (j)	0.0	$0 \leq j \leq 2$

Here follows a sequence of comparison between the results of a full finite differences scheme and a mixed pseudospectral-finite difference method [Bueno-Harris].

In the following Figure 2 the profiles are presented in three of five periods of the process. Initial time condition is a constant concentration of oxygen based on capillary conditions for a sickle and normal cell. The second case of each profile set shows a middle path situation and the last case is the final RBC membrane deformation and oxygen concentration profile at the end of the capillary.

Cases	Tekleab-Harris Model	Filho-Harris Model
Lx = 10, Elliptical Initial RBC Geometry - Normal Case, J = 0		
Case 1 T = 0	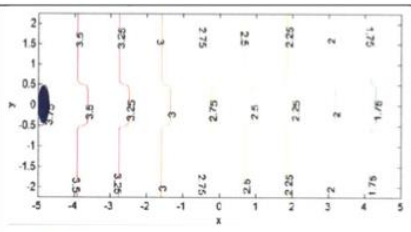	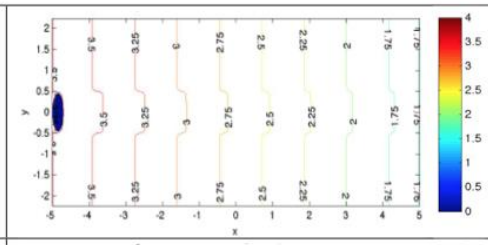
Case 2 t = 2	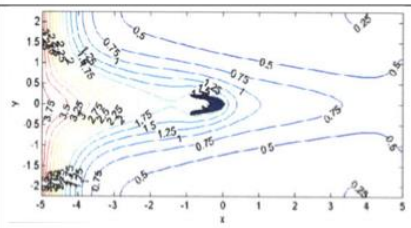	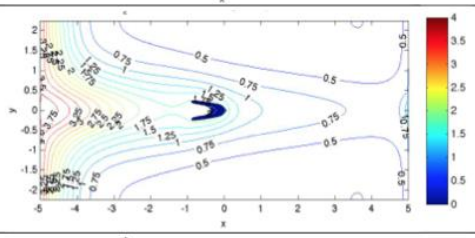
Case 3 t = 4	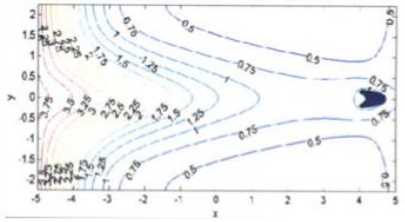	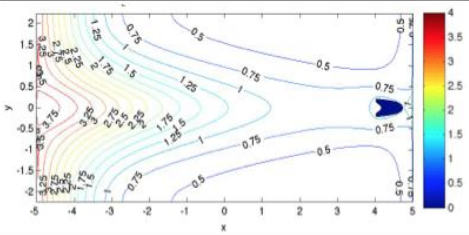
Lx = 10, Elliptical Initial RBC Geometry - Sickle Case, J = 0		
Case 4 t = 0	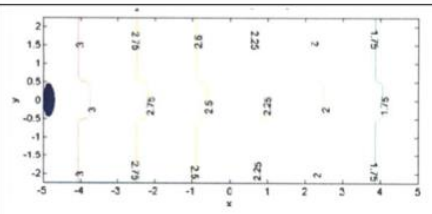	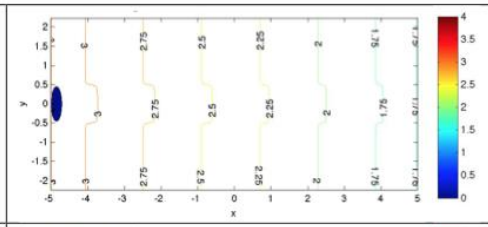
Case 5 t = 2	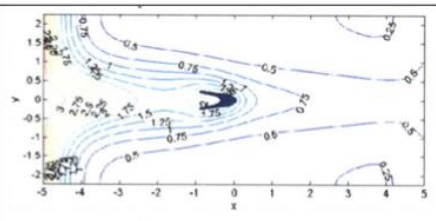	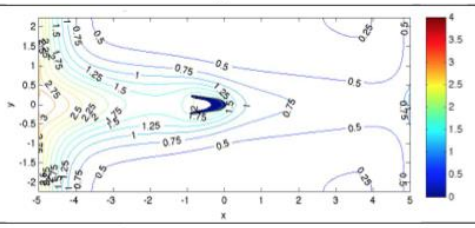
Case 6 t = 4	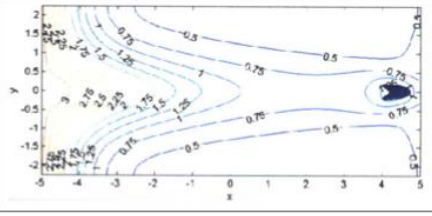	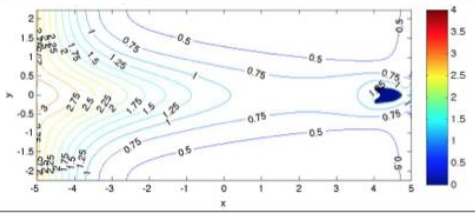

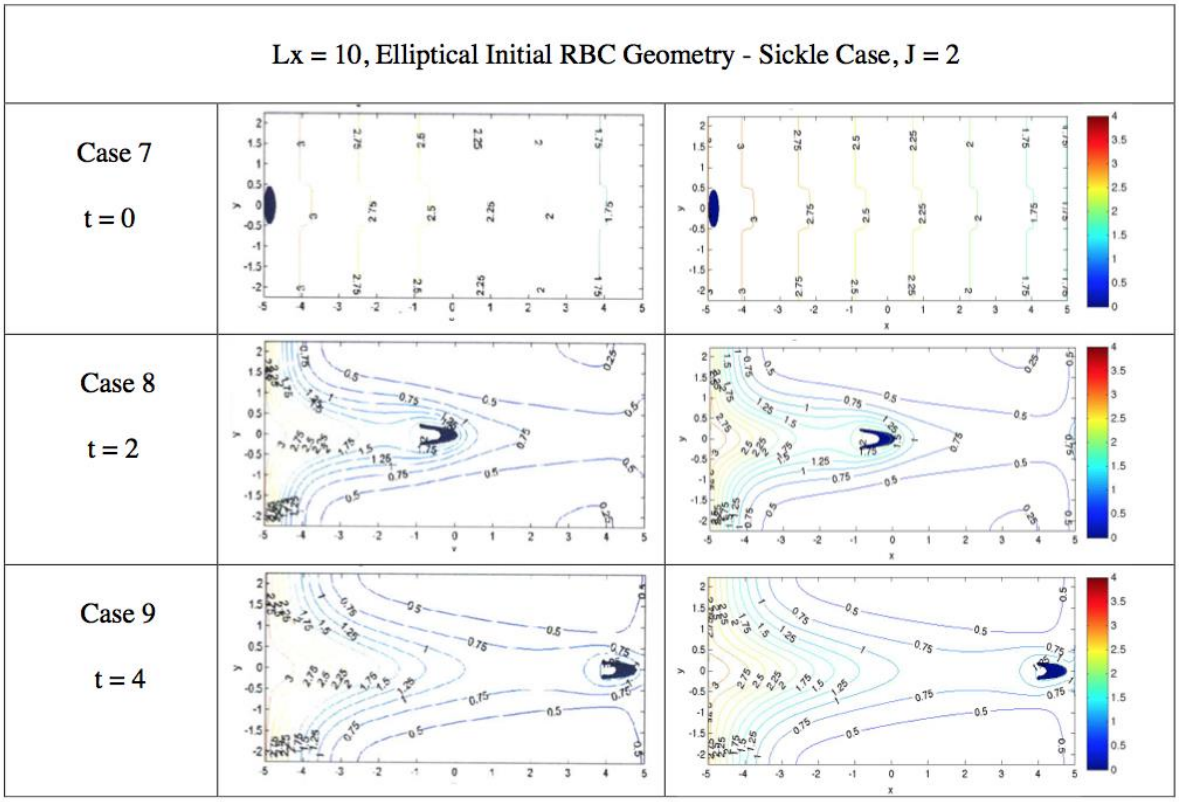

Figure 2: Oxygen Profile Comparison

This first group of cases covers the analysis of the oxygen concentration profile from the RBC membrane, through the blood plasma and into the surrounding tissue. The capillary is represented for a tube of 10 units of measure of length and 4 units of width representing the surrounding tissue.

The consistency of Bueno-Harris model with the Harris-Tekleab results is noted. The initial elliptic RBC shape and its membrane deformation in a "bullet" shape coupled with the variation in the oxygen profile concentration were expected. Also, the non-intuitive scenario, of higher values of oxygen near the cell as time elapse, can be highlighted. This is a straightforward result of a correct development of the blood plasma flow in pseudospectral method and an appropriate connection between the myoglobin, hemoglobin and oxygen concentration implementation.

The cases 1, 4 and 7 for both models are exactly the same due to the constant initial concentration of oxygen for normal and sickle microcirculation condition. In the cases 2, 3, 5, 6, 8 and 9 it is possible to see a slightly different oxygen concentration drop (less significant) in Bueno-Harris model, mainly in the boundaries. However, there is similarity with the Tekleab-Harris model with respect to the oxygen concentration profile, RBC membrane deformation and the values of the oxygen concentration.

In this case 9 is noted that not only a stretched RBC shape in Teakleab-Harris profile, but also a stretch oxygen profile in the Bueno-Harris results. This can be explained by the north and south clustered Chebyshev collocation and west and east periodicity of the Fourier-spectral scheme.

An other test case to validate the physics of the problem is the capture of weak vortices. These perturbations happen due to the jump pressure across the membrane of the RBC, where the V velocity

profile depicts those small eddies. As the jump pressure formulation depends on the stress on the RBC membrane, which is assumed a linear relation with curvature as follows:

$$\sigma = K_{RBC} k \quad (17)$$

where the curvature k is given by :

$$k = \frac{\phi_{xx}\phi_y^2 - 2\phi_x\phi_y\phi_{xy} + \phi_{yy}\phi_x^2}{\left(\phi_x^2 + \phi x_y^2\right)^{\frac{2}{3}}} \quad (18)$$

where $\phi(x, y)$ is a function that defines the boundary between the membrane and the plasma.

Therefore, the greatter effects of this phenomenon are presents at the ends of the RBC as shown in figure 3.

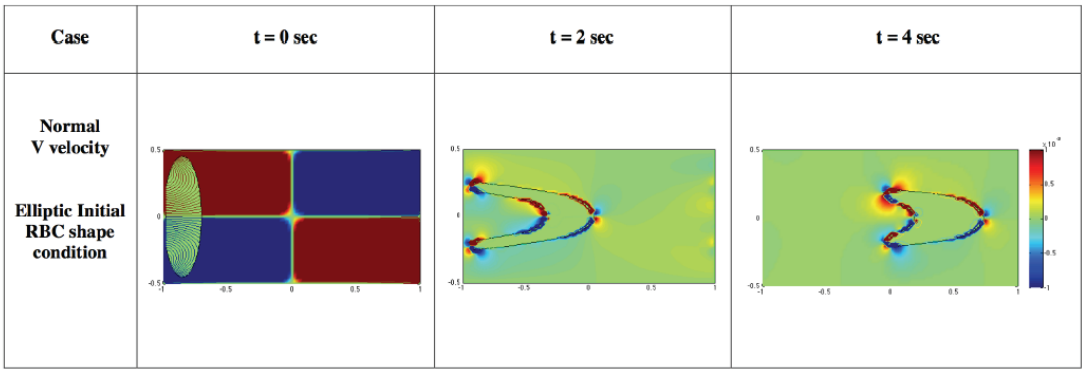

Figure 3: V velocity profile and small eddies.

Those small eddies, which are reflected in the V velocity, are also the result of the RBC inside the simple Poiseuille flow that would have a V velocity component equals to zero in anywhere.

5 Conclusion and Future Work

The pseudospectral scheme to mathematically simulate the blood plasma flow appears to be a promising feature to be used. An appropriate change in the oxygen concentration profile for each microcirculation scenario corresponds to our expectation. Also, the non-intuitive higher oxygen concentration values in the tissue and roughly in whole plasma for a normal cell when compared to a sickle one. Computationally speaking, due to the tensor product, this model has a higher computational cost, but due to the spectral accuracy, it exceeds the finite differences scheme in this sense, since the profiles converge exponentially.

However, there are some limitations that is not related to the accuracy of the method, for this reason, other implementation of this model should be considered in a future work. In order to reach a better mathematical model of this microcirculation problem, the discrete Navier-Stokes equation should be in a cylindrical form. Another interesting implementation is to simulate the RBC membrane

deformation with Immersed Boundary Method, instead level set method. In this case, equation (2) has a force term that automatically carries the influence of the RBC shape modification into the velocity, and pressure, avoiding the approximation of the jump condition at RBC for correction of pressure and velocity, saving computational time and reducing cost. Moreover, the pseudospectral implementation of equation (3) will allow a better compatibility between the blood plasma flow, membrane deformation and oxygen concentration.

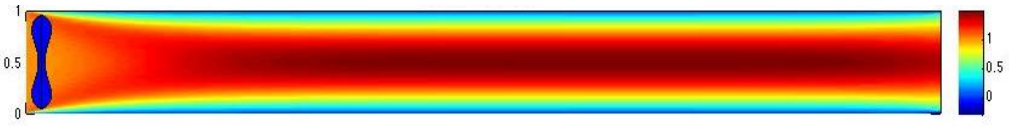

Figure 4: Bi-concave RBC Initial geometry in a capillary

.

For a better representation of this specific problem, the Figure 3 depicts an initial bi-concave RBC geometry into the blood plasma flow, which can guarantee results closer to those obtained for Le-Floch-Yin [2] in his three dimensional model. Additional research is required to find a different stress function, which should not be direct proportional to the curvature of the RBC as it is for an elliptical initial geometry. On the other hand, it is a fact that this improvement would maximize the overall stress on the cell membrane creating results that can compare with a two-dimensional moving mesh model.

These improvements to the Bueno-Harris model would allow an accurate and low cost code to be used in a preliminary study of the sickle cell disease.

References

[1] Y. Tekleab, and W. L. Harris, A Two-Dimensional Model of Blood Plasma Flow with Oxygen Transport and Blood Cell Membrane Deformation, ICCFD7-3205.2012

[2] F. Le Floch-Yin. *Design of a Numerical Model for Simulation of Blood Microcirculation and Sickle Cell Disease.* (Ph.D. Thesis – Department of Aeronautics and Astronautics). MIT. 2010.

[3] Y. Tekleab. *A perturbation Model for Normal and Sickle Cell Blood Microcirculation.* (M.S. Thesis – Department of Aeronautics and Astronautics). MIT. 2011.

[4] Roger Peyret. *Spectral Methods for incompressible viscous flow,* volume 148 of *Appl. Math. Sci.* Springer, 2002.

[5] David Gottlieb and Steven A. Orszag. *Numerical analysis of spectral methods: theory and application.* Regional conference series in applied mathematics. SIAM, 1977.

[6] L.N. Trefethen. *Spectral Methods in Matlab.* SIAM, 2000.

[7] S. A. Berger and W. S. King. *The Flow of Sickle Cell Blood in the Capillaries*, Biophysical J., 29(1); 11-148. 1980.